Tenth International Conference on Computational Fluid Dynamics (ICCFD10), Barcelona, Spain, July 9-13, 2018

ICCFD10-165

Coupled Simulation of Flow–particle–structure Interaction of Shot Peening Process by Immersed Boundary Method and Finite Element Method

Y. Mizuno*, T. Kubota*, S. Takahashi*and K. Fukuda*
Corresponding author: 7btad010@mail.u-tokai.ac.jp

* Tokai University, Japan

Abstract: We developed a flow–structure coupling solver based on immersed boundary method (IBM) and finite element method (FEM) and investigate a flow around cylinders falling, colliding with a structure and rebounding. In this study, all objects which are cylinders and structure are defined by the level–set function for ghost–cell method of IBM. The movement of cylinders is described by the equations of motion for xy–transportations. The flow–structure coupling is solved by using loosely coupling method. As results, the impact velocity of cylinder is affected by the movement of pre– and post– collision and the wake vortices of other cylinder. The stress and the plastic strain generated in the structure showed the different distributions with each collision point.

Keywords: Flow–structure Coupling Simulation, Immersed Boundary Method, Multiple Cylinder–structure Collisions.

1 Introduction

Shot peening process is exploited to impact material surface with a large number of small particles for generating a compressible residual stress on the surface. The strength of structure is enhanced by this process. The interaction of flow–particles, particles–structure and structure–flow can be key roles for more accurate and efficient process. In the flow–particles interaction, the freestream from nozzle and vortices affect the motion of particles such as the falling, rebounding and colliding. In the particles–structure interaction, the residual stress is generated on the structure surface by the impact with particles and, the energy of particle is lost by this impact. In structure–low interaction, the transformation of surface shape affects the flow fields. Nguyen et al. [1] investigated the location of particles–surface impacts by using commercial flow solver. They used the Euler–Lagrange approach and Reynolds–averaged Navier–Stokes equations (RANS), which cannot sufficiently model the particle–flow interactions and the detailed flow structures. Tu et al. [2] explored the residual stress by using commercial flow–structure solver. They utilized the discrete element model (DEM) and finite element model (FEM). The previous studies by using numerical simulations are conducted for a steady flow and based on the one–way coupling scheme which ignored the interaction between flow–particles. We developed the two– and three–dimensional Euler–Euler flow solvers based on an immersed boundary method (IBM) because of examining the interaction of flow–particles [3, 4, 5]. The IBM developed by Mittal et al. [6] is widely used for its simplicity and applicability to the moving and multiple objects. This study is devoted to investigate flow–structure coupling phenomena based on IBM and FEM by using two–dimensional loosely coupling solver.

2 Computational Method

2.1 Flow Solver

Governing equations are two–dimensional incompressible Navier–Stokes equations, an equation of continuity and an equation of motion for two–degrees of freedom. No averaging and filtering processes are involved in this simulation:

$$\frac{\partial u}{\partial t}+u\frac{\partial u}{\partial x}+v\frac{\partial u}{\partial y}=-\frac{1}{\rho}\frac{\partial p}{\partial x}+\nu\left(\frac{\partial^2 u}{\partial x^2}+\frac{\partial^2 u}{\partial y^2}\right),$$
$$\frac{\partial v}{\partial t}+u\frac{\partial v}{\partial x}+v\frac{\partial v}{\partial y}=-\frac{1}{\rho}\frac{\partial p}{\partial y}+\nu\left(\frac{\partial^2 v}{\partial x^2}+\frac{\partial^2 v}{\partial y^2}\right), \quad (1)$$

$$\frac{\partial u}{\partial x}+\frac{\partial v}{\partial y}=0, \quad (2)$$

where u, v, p, ρ and ν are the fluid velocity, pressure, density and kinematic viscosity, respectively. The fractional step method is applied for time marching. The grid is defined by an equally spaced Cartesian mesh. The convection term is evaluated by the second–order skew–symmetric scheme. The pressure and diffusion terms are calculated by the second–order finite–difference method. Poisson equation of the pressure is calculated by the successive over–relaxation (SOR) method. The objects are represented by the level set method and the ghost cell method [3, 4, 5]. The aerodynamic pressure and friction forces acting on the object surface are calculated on the cell face between the fluid and ghost cells. In the present method, the forces are estimated by a simple algorithm using a staircase representation, which negates the need for surface polygons [8]. The object movement is expressed by the equations of motion for xy–transportations.

2.2 Structure Solver

The FEM solver is developed based on the plane strain model. The element is evaluated by the 8–nodes iso–parametric rectangular elements. The failure criterion is stated by the Von–Mises criterion. The stiffness equations including the inertial force described by

$$[M]\{\ddot{u}\}+[K]\{u\}=\{\dot{F}\}, \quad (3)$$

where $[M]$ and $[K]$ are the lamped mass matrix and the global stiffness matrix. In finding the solutions, the equations are solved for global displacement velocity increment vector $\{\ddot{u}\}$ as differential equation of global displacement velocity vector $\{u\}$ given by

$$\ddot{u}_n=\frac{u_{n+1}+u_{n-1}-2u_n}{\Delta t^2}, \quad (4)$$

where Δt is the time increment. Finally, the equation given by

$$\{u_{n+1}\}=\Delta t^2[M]^{-1}\left[\{\ddot{F}_n\}-[K_n]\{u_n\}\right]+2\{u_n\}-\{u_{n-1}\}, \quad (5)$$

where n is time step.

The external force distribution and the collision time are defined by the Hertz theory model.

2.3 Flow–Structure Coupling Method

The flow–structure coupling is solved by using loosely coupling method. In the flow–particles interaction, the aerodynamic forces affect the particles, and the vortices are generated by the moving particles. In the particles–structure interaction, the impact of particles contributes an external force to the structure. Conversely, the particles receive the reaction force from the structure. In the structure–flow interaction, the transformation of surface shape changes the flow fields. In flow simulation, the transformation of structure is represented by the level set function. In the flow simulation, the data of colliding location and external force pass to structure simulation at step of collision between particle and structure. The time increment of flow simulation is calculated based on the maximum velocity of fluid and cylinder at every step. The structure simulation is performed when the cylinder collides with

the structure and is repeatedly conducted several times during the flow simulation. At the colliding time step, the number of time steps and time increment of structure simulation are defined based on the cylinder–structure contact time. After next time step, the number of steps and time increment are defined based on the time increment of flow simulation.

3 Computational Result

3.1 Flow around a Falling Cylinder with a Structure

3.1.1 Condition

The flow–structure coupling solver is applied to the flow around a cylinder falling, colliding with the surface of metal structure and rebounding and the structure model as steel.
Figure 1 shows the computational domain. The cylinder diameter is set to be $D = 8\times10^{-6}$ m. The computational mesh sizes of flow simulation and structure simulation are fixed at $dx_f = D / 40$ and $dx_s = D / 20$, respectively. The computational domains of flow simulation and structure simulation are set to be $8D \times 11.25D$ and $8D \times 3D$, respectively. The Reynolds numbers based on the cylinder diameter and the relative velocity between the freestream and the cylinder velocity at its impacts the wall are set to be 400 (case1–1) and 600 (case1–2), respectively. The material of cylinder is set to be a rigid body of alumina. The Young's modulus, yield strength and density of structure are 206 GPa, 500MPa and 7800 kg/m^3, respectively.

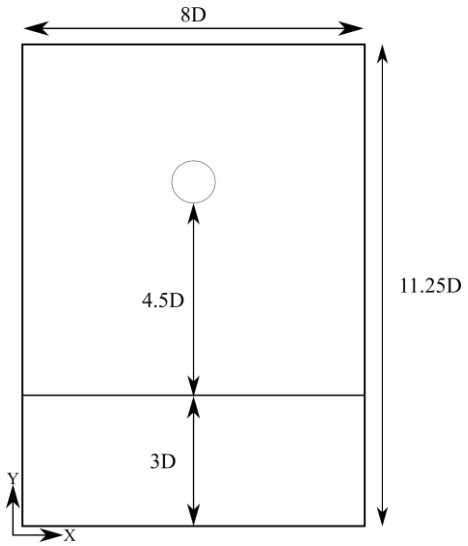

Figure 1: Computational domain (D is cylinder diameter).

3.1.2 Result

Figure 2 shows the instantaneous flow distributions visualized by the velocity (left images) and the vorticity (right images) in the case 1–1. The cylinder collides with the structure at nondimensional time $t^* = 4.5$ (Fig. 2 (b)). The vortices are generated between the cylinder and structure and on the surface of structure. The cylinder rebounds from the structure at $t^* = 4.6$ and the vortices formed around the cylinder become reversed (Fig. 2 (c)). The vortices are generated behind of the cylinder due to the relative velocity between the freestream and the cylinder velocity (Fig. 2 (d)–(f)). The vortices on the surface of structure are influenced by the freestream and cylinder. In this simulation, almost the same distribution is obtained between the case 1–2 and case 1–1.
Figure 3 plots the cylinder velocity normalized by freestream, where the red and blue lines show the case 1–1 and case 1–2, respectively. The cylinder velocity becomes reversed by the collision (Fig. 3 (a)). The falling cylinder velocity is decreased by the freestream curled up (Fig. 3 (b)). In the case 1–1, the influence is enhanced than one in the case 1–2. In Fig. 3 (c), the rebounding cylinder velocity decreases more than in Fig. 3 (b) because the cylinder directly received the influence of the freestream

at rebounding. The drag force in the case 1–1 becomes larger than in the case 1–2. Thus the cylinder velocity in the case 1–1 decreases more than one in the case 1–2. The cylinder velocity at the collision decreases sharply because the energy of cylinder is lost by the collision.
Figure 4 shows the instantaneous strain distribution at collision between the cylinder and the structure. At the collision, the stress is generated in the structure. The value of stress in the case 1–2 is larger than in the case 1–1 because the impact energy and the collision time are large. As a result, the large plastic strain is formed in Fig. 5. The impact energy is lost by the plastic strain; the cylinder velocity is decreased in Fig. 3 (c).

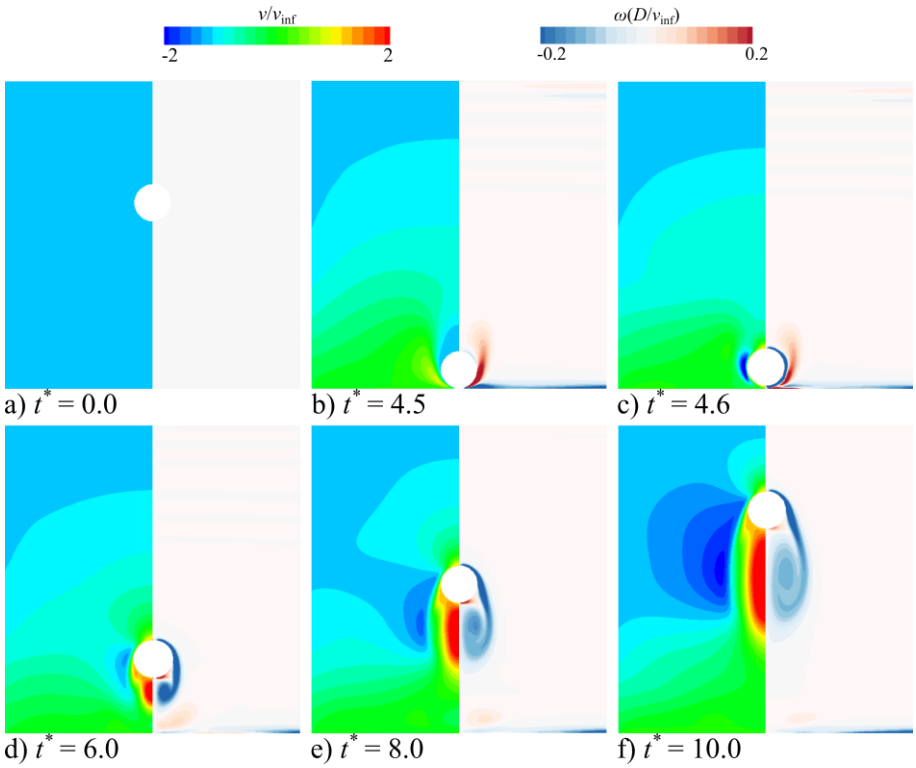

Figure 2: Instantaneous distributions visualized by velocity (left images) and vorticity (right images) in case1–1.

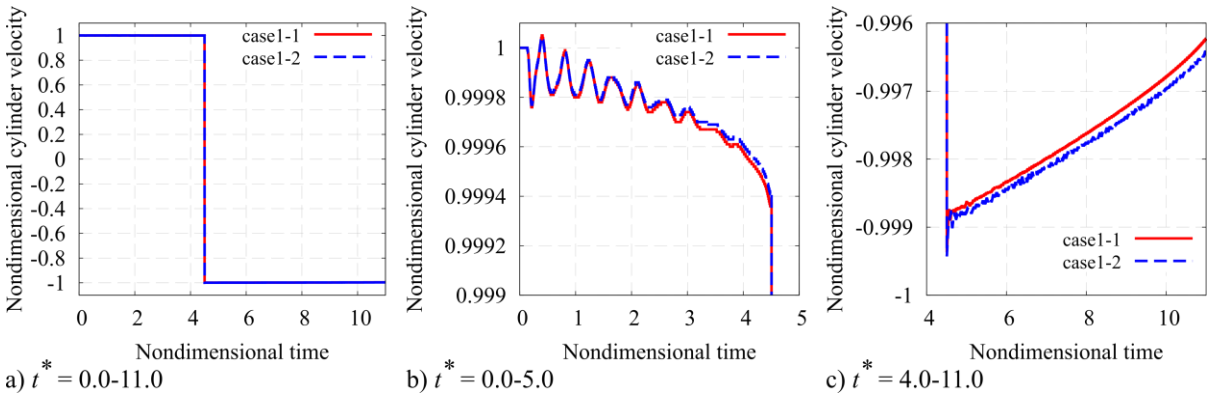

Figure 3: Variation cylinder velocity.

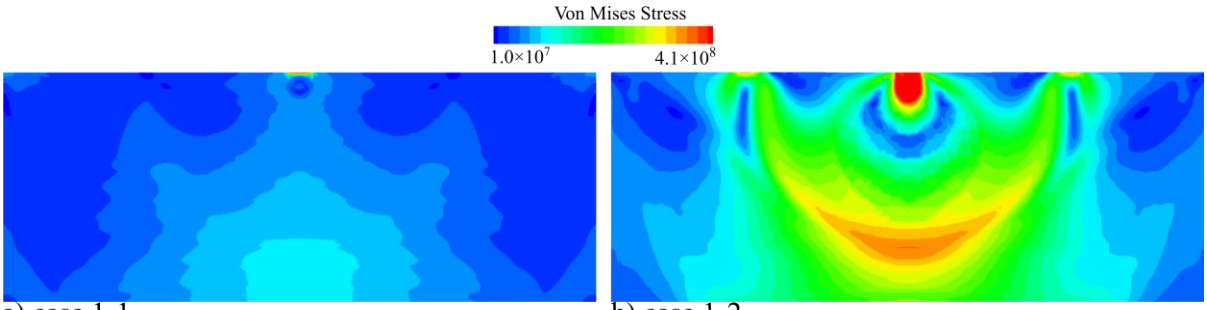

Figure 4: Instantaneous stress distributions after the collision between the cylinder and the structure.

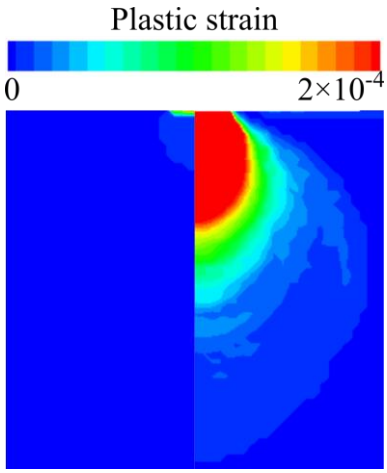

Figure 5: Plastic strain at collision point in case 1–1 (left image) and case 1–2 (right image).

3.2 Flow around Falling Five Cylinders with a Structure

3.2.1 Condition

The flow–structure coupling solver is applied to the flow around five cylinders falling, colliding with the surface of metal structure and rebounding and the structure model as steel.

Figure 6 shows the computational domain. The cylinder diameter is set to be $D = 8\times10^{-6}$ m. The computational mesh sizes of flow simulation and structure simulation are fixed at $dx_f = D / 40$ and $dx_s = D / 20$, respectively. The computational domains of flow simulation and structure simulation are set to be $8D \times 11.25D$ and $8D \times 3D$, respectively. The five cylinders are arranged as Figure 6. The three cylinders (N1–N3) are set to collide with the structure at first. After that, the rest of two cylinders (N4 and N5) collide with the structure. The Reynolds numbers based on the cylinder diameter and the relative velocity between the freestream and the cylinder velocity at its impacts the wall are set to be 400 (case 2–1) and 600 (case 2–2), respectively. The material of cylinder is set to be a rigid body of alumina. The Young's modulus, yield strength and density of structure are 206 GPa, 500MPa and 7800 kg/m^3, respectively.

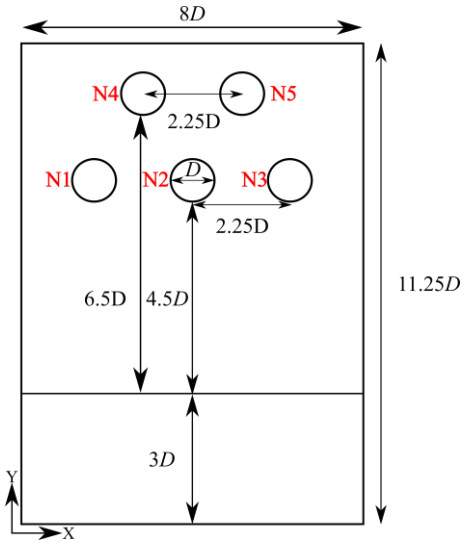

Figure 6: Computational domain (*D* is cylinder diameter).

3.2.2 Result

Figure 7 and 8 show the instantaneous vorticity distributions in the case 2–1 and velocity distributions in the case 2–2. Three cylinders (N1–N3) collide with the structure (Fig. 7 and 8 (b)). The wake vortices are formed from N1 and N3 because of the two cylinders behind. The N4 and N5 pass between the N1–N3 rebounded (Fig. 7 and 8 (c)). Each cylinder interferes with the wake vortices of other cylinders. N4 and N5 collide with the structure (Fig. 7 and 8 (d)). The wake vortices of N4 are the same pattern with one of N5. All the cylinders rebound (Fig 7 and 8 (e)). The wake vortices of N1 and N3 are enfolded in one of N4 and N5. The flow near the wall becomes complex by the interaction between the vortices and cylinders.

Figure 9 and 10 plot the cylinder velocity normalized by one of the freestream in the case 2–1 and the case 2–2, where the case 1–1 and case 1–2 are shown in black lines as references. N2 shows the same tendency with case 1–1 firstly (Fig 9 (a)); N2 shows the same initial position and initial velocity with the case 1–1 and case 1–2, respectively. In the vicinity of the wall, however, the decrease of the cylinder velocity of N2 is larger than one in the case 1–1 and case 1–2, respectively. The cylinder velocities of N1–N3 are influenced by the N4 and N5. When N4 and N5 pass between N1–N3 rebounding, particle velocities are increased temporarily by the wake vortices of N1–N3. This variation of the case 2–1 is smaller than one of the case 2–2 due to the different Reynolds number. After N4 and N5 move behind N1–N3, particles velocities decrease again. This nonlinear phenomenon becomes important factor about the impact velocity of the cylinder. The gradients of velocities of N1–N3 of the case 2–1 and case 2–2 become larger than on of the case 1–1 and case 1–2, respectively (Fig. 9 and 10 (c)). N4 and N5 gradually decelerate by the influence of wake vortices of N1–N3. The impact velocity (minimum velocity in Fig. 9 and 10 (c)) of N4 and N5 in the case 2–1 becomes smaller than one of N1–N3. However, the impact velocity in the case 2–2 becomes larger than one of N1–N3. This value of impact velocity is influenced by the phenomena of pre–collision.

Figure 11 shows the instantaneous strain distribution at first collision time $t^* = 4.5$ (panel (a) and (c)) and second collision time $t^* = 7.0$ (panel (b) and (d)). The stress distribution becomes symmetry. The stress on the collision points of N2 is smaller than one of N1 and N3 because the stress wave interact at $t^* = 4.5$. The stress distribution becomes more complex at $t^* = 7.0$. The plastic strain is affected by the adjacent plastic strain in Fig. 12. The plastic strain of N4 and N5 become smaller than one of N1–N3 because the impact velocity is smaller.

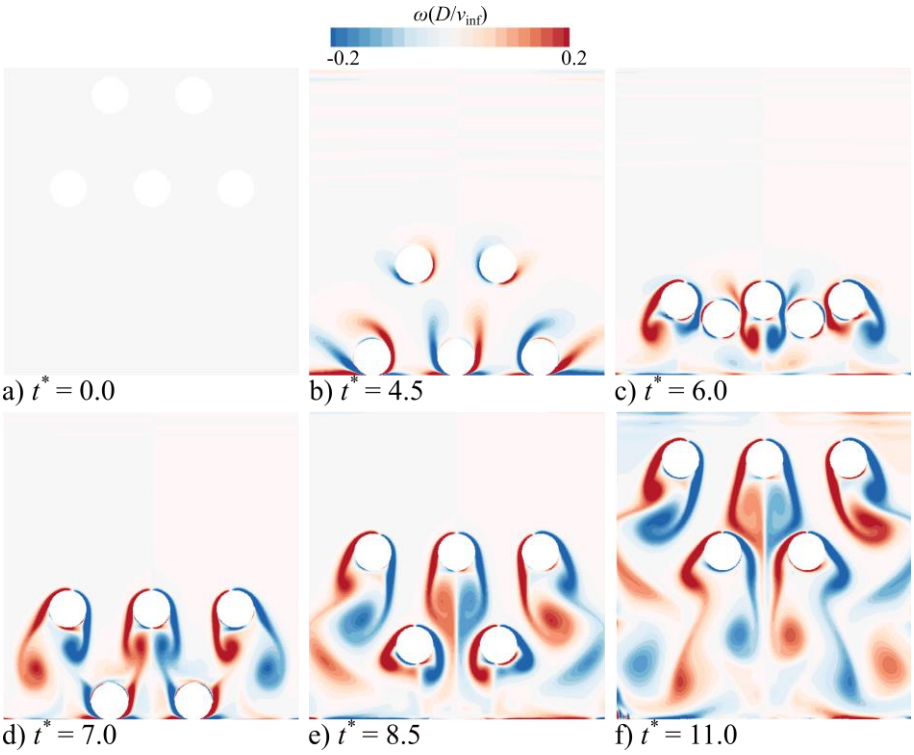

Figure 7: Instantaneous vorticity distributions in case 2–1.

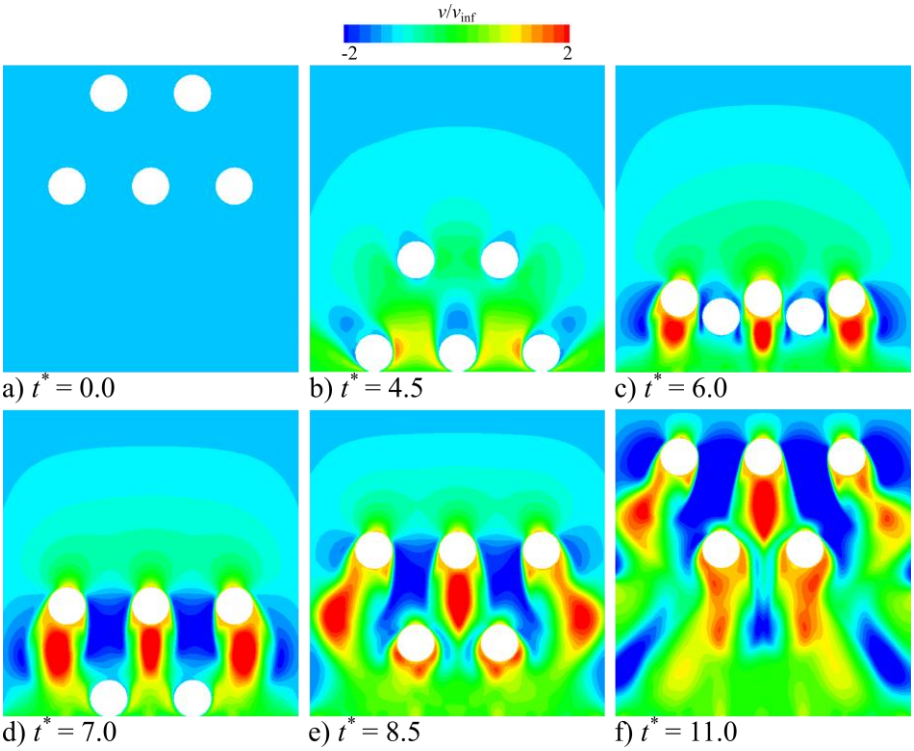

Figure 8: Instantaneous velocity distributions in case 2–2.

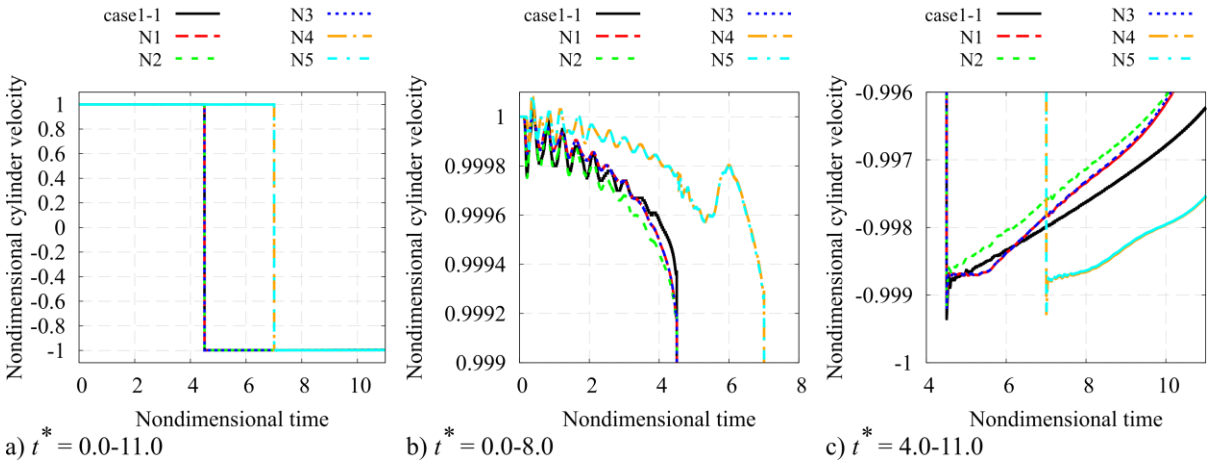

Figure 9: Variation cylinder velocity in case 2–1.

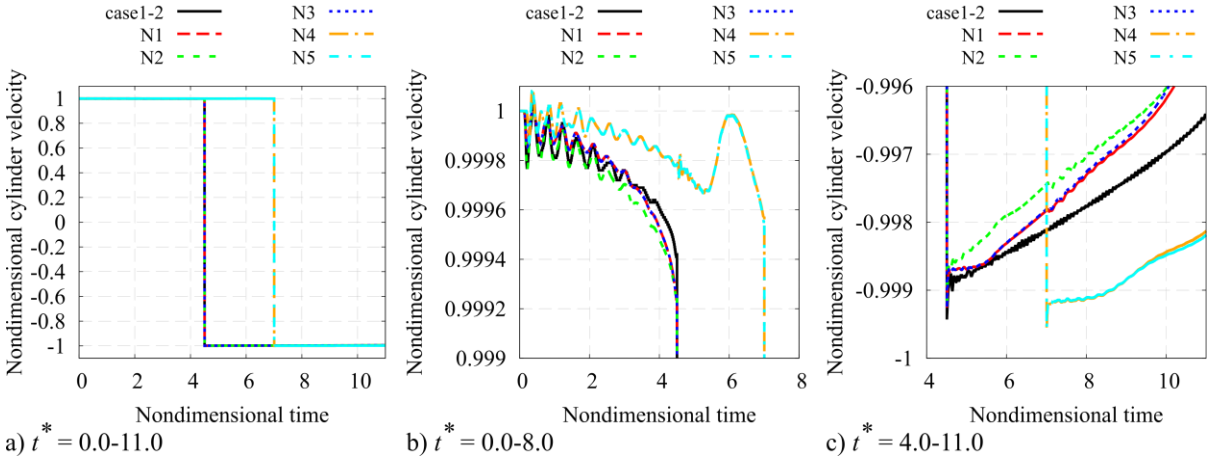

Figure 10: Variation cylinder velocity in case 2–2.

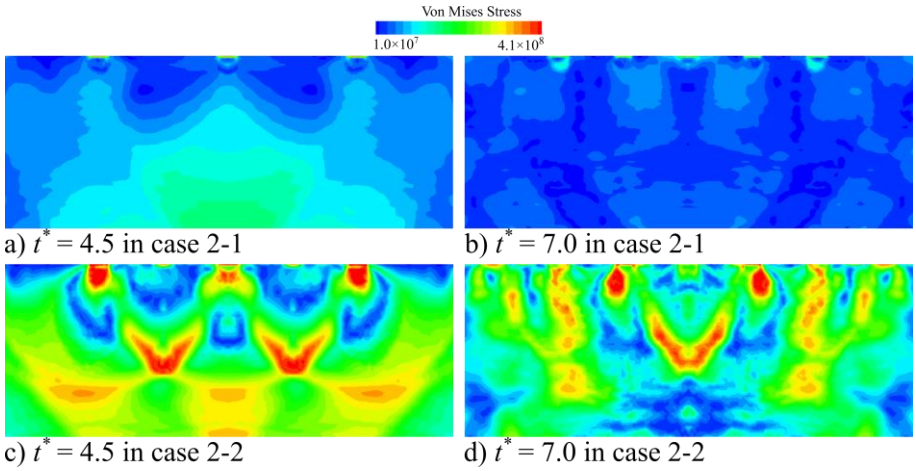

Figure 11: Instantaneous stress distributions after the collision between the cylinder and the structure.

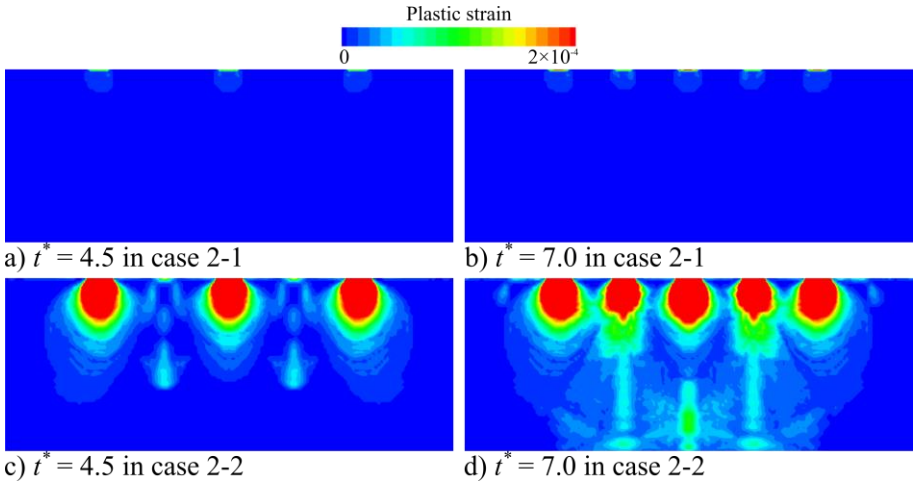

Figure 12: Plastic strain.

3 Conclusions and Future Works

A flow–structure coupling simulation was conducted by using IBM–FEM coupled solver. We investigated a flow around one to five cylinders falling, colliding with a structure of metal and rebounding. The main results are summarized below:

(1) At Reynolds numbers 400 and 600, the flow phenomenon around the cylinders and the structure was almost the same. However, the stress and the plastic strain in the structure showed the different distribution due to the different impact velocity of cylinder.

(2) In five cylinders case, the wake vortices of cylinders became complex during the rebounding by the interaction with other cylinders.

(3) The cylinder velocity of pre–collision with the structure became the nonlinear by the interaction between the vortices and cylinders. Moreover the nonlinear change shown a different trend based on Reynolds number.

(4) The stress and the plastic strain generated by the collision interfered with the stress and the plastic strain generated by other collisions. They were affected by the impact velocity of cylinder.

In future work, we develop three–dimensional flow–structure coupling solver to investigate a flow around multiple particles and a structure.

Acknowledgments

The computations are carried out by NEC SX-9 and SX-ACE at Cyberscience Center and Institute of Fluid Science (IFS) of Tohoku University with the resources of High Performance Computing Infrastructure (HPCI) hp150130, hp160150, hp170111 and collaborative researches with IFS. This work was supported by JSPS KAKENHI Grant Number 16K18018 and 18K03937.

References

[1] V. B. Nguyen, H. J. Poh, and Y. W. Zhang. Predicting shot peening coverage using multiphase computational fluid dynamics simulations. Powder Technology, 256: 100-112, 2014.

[2] F. Tu, D. Delbergue, H. Miao, T. Klotz, M. Brochu, P. Bocher and M. Levesque. A sequential DEM-FEM coupling method for shot peening simulation. Surface and Coatings Technology. 319: 200-212, 2017.

[3] S. Takahashi, T. Nonomura and K. Fukuda. A Numerical Scheme Based on an Immersed Boundary Method for Compressible Turbulent Flows Shock Application Two-dimensional Flows around Cylinders. Journal of Applied Mathematics, 2014.

[4] Y. Mizuno, S. Takahashi, T. Nonomura, T. Nagata and K. Fukuda. A Simple Immersed Boundary Method for Compressible Flow Simulation around a Stationary and Moving Sphere. Mathematical Problem in Engineering. 1-17, 2015.
[5] Y. Mizuno, T. Inoue, S. Takahashi and K. Fukuda. Investigation of A Gas-particle Flow with Particle-particle and Particle-wall Collisions by Immersed boundary Method. 6: 132-138, 2018
[6] R. Mittal and G. Iaccarino. Immersed Boundary Methods. Annual Review of Fluid Mechanics, 37: 239-261, 2005.
[7] T. Nonomura and J. Onishi. A Comparative Study on Evaluation Method of Fluid Force on Cartesian Grids. Mathematical Problems in Engineering, 2017.